Iranian Journal of Hydrogen & Fuel Cell

IJHFC

Journal homepage://ijhfc.irost.ir

Exergy analysis of a molten carbonate fuel cell-turbo expander-steam turbine hybrid cycle

H. A. Ozgoli*

Department of Mechanical Engineering, Iranian Research Organization for Science and Technology (IROST), Tehran, Iran

Abstract

Exergy analysis of an integrated molten carbonate fuel cell-turbo expander-steam turbine hybrid cycle has been presented in this study. The proposed cycle has been used as a sustainable energy approach to provide a micro hybrid power plant with high exergy efficiency. To generate electricity by the mentioned system, an externally reformed molten carbonate fuel cell located upstream of the combined cycle has been used. Furthermore, the turbo expander and steam turbine systems have been considered as topping and bottoming cycles for the purpose of cogeneration, respectively. Results show that the proposed system is capable of reaching a net delivered power of 1125 kW, while the total exergy efficiency (including both electricity and heat) of this system is more than 68%. Moreover, the delivered power and exergy efficiency from the proposed cycle is stable against ambient temperature variations. In addition, the effect of a current density increase on cell voltage and total exergy destruction has been considered.

1. Introduction

Enormous attention is being given to reduce greenhouse gasses and other pollutants into the atmosphere by developing suitable technologies for the efficient conversion of traditional as well as renewable sources to meet growing energy demand.

Since fuel cells are not "Carnot limited" they are high efficiency energy conversion devices. Two types of high temperature fuel cells are the solid oxide fuel cell (SOFC) and molten carbonate fuel cell (MCFC) with an operating temperature between 600°C and 800°C [1].

Hybrid systems based on high temperature fuel

cells coupled to a gas turbine cycle can be an alternative approach to supply the required fuel of power generators from a sustainable view point. In addition, the MCFC generator can be synergistically integrated with a gas turbine (GT) engine, since the temperature of MCFC exhaust gas is generally high. Thus, various types of integration of high temperature fuel cells (SOFCs, MCFCs) and conventional power generators combined as heat and power (CHP) systems have been proposed and implemented [2-6]. Many studies conducted on MCFCs show that integrating MCFCs with gas turbine systems for power generation increases the efficiency and the overall performance of the hybrid system.

Some of these related studies have been shown in Table 1.

Leto et al. [21] modeled a hybrid system consisting of a MCFC coupled with a micro-turbine, and performed a sensitivity analysis by varying the main operating parameters. They demonstrated that this system could reach electrical and overall efficiencies up to 60% and 70%, respectively. El-Emam and Dincer [22] conducted energetic and exergetic analyses of an MCFC-GT system and obtained overall energetic and exergetic efficiencies of 42.9% and 37.75%, respectively. (the table should not be inside the sentence, but above its label).

Table 1. Output power and total efficiency of some combined MCFC-GT systems

Hybrid Cycles	Output Power	Total En./Ex. Eff.	Ref.
MCFC–GT	418.2 kW	56.16% (Ex. Eff.)	[7]
MCFC–GT	568.3 kW	75.6% (En. Eff.)	[8]
MCFC–GT-ST	63.2 MW	53.8% (En. Eff.)	[9]
MCFC–TE	2.2 MW	65.0% (Ex. Eff.)	[10]
MCFC–GT-ST	505.9 kW	58.88% (En. Eff.)	[11]
MCFC–GT	463 kW	41.1% (En. Eff.)	[12]
GT-MCFC	2.259 MW	88.8% (En. Eff.)	[13]
MCFC–GT	148.8 kW	56.6% (En. Eff.)	[14]
MCFC–GT	600.0 kW	74.0% (En. Eff.)	[15]
MCFC–GT	147.8 kW	58.53% (En. Eff.)	[16]
MCFC–GT	1250 kW	74.4% (En. Eff.)	[17]
MCFC–GT	20 MW	69.5% (En. Eff.)	[18]
MCFC–GT	303 kW	52.0% (En. Eff.)	[19]
MCFC–GT	350 kW	42.0% (En. Eff.)	[20]

Rashidi et al. [23] conducted a similar study on an MCFC-Gas turbine system and achieved an overall energetic efficiency of 57.4%, exergetic efficiency of 56.2%, bottoming cycle energetic efficiency of 24.7%, and stack energetic efficiency of 43.4%. Chacartegui et al. [24] presented a MCFC combined with a STIG cycle, which operated at ambient pressure. Their examination showed the efficiency up to 69%. An exergy based thermodynamics analysis was performed by Haseli et al. [25] to study the performance of a combined SOFC-GT system for power generation. The energy and exergy efficiencies calculated were 60.6% and 57.9%, respectively. In another research, it was observed that a MCFC with 46.4% efficiency has the capability of being integrated with a steam generation power system in order to achieve an overall efficiency of nearly 70% [26]. Haghighat Mamaghani et al. [27] presented a multi-objective optimization on a MCFC-GT hybrid system with 200 kW capacity. Their work expressed the overall exergetic efficiency of 51.7% for this system.

Although many works have been carried out on modeling and optimization of MCFC based hybrid plants, no thorough study from thermal and environmental viewpoints has been performed.

Applying the second law of thermodynamics, with the exergy concept, while studying the overall plant performance is very important to know the extent of losses within the system. Moreover, the exergy based thermodynamic analysis is believed to lead to more sustainable development.

Motivated by this research gap, the present study first developes a new comprehensive thermodynamic model of a hybrid MCFC-turbo expander (TE)-steam turbine (ST) plant and then evaluates the behavior of the system from an exergetic standpoint. A parametric study is also performed to investigate the effects of varying operating parameters on the system efficiencies and exergy destructions. Additionally, based on a greenhouse gas emission point of view, environmental aspects of the proposed hybrid cycle have been studied in this paper.

2. System configuration

A schematic of the proposed system has been shown in Fig. 1. The pressurized MCFC, used at the upstream of the MCFC to convert natural gas into H_2, operates with an external steam reformer. Before being fed to the MCFC cathode heat recovery, natural gas is heated in a heat exchanger using the hot exhaust stream of the steam reformer. Steam required for the reforming reaction is produced in a heat exchanger using the hot streams leaving the reformer and cathode of MCFC.A combustor is used downstream of the MCFC, where the remaining fuel in the anode exhaust stream is combusted. The resulting anode flue gas is fed to the reformer which supplies the heat required for the endothermic reactions occurring inside the steam reformer.

During operation CO_2 is concentrated at the anode of the MCFC. The anode exhaust stream is therefore rich in CO_2 but also it has a large amount of steam. A moisture separator is used downstream of the MCFC to further enrich the anode exhaust stream with CO_2 by condensing some steam in it. The moisture separator supplies the heat, extracted from the anode exhaust stream, to a stream of recirculated cold water. The heat of this recirculated hot water is then absorbed in a heat sink for other purposes such as cogeneration. Then the pressured hot exhaust gasses from the MCFC cathode flows into the turbo expander to generate power. In a heat recovery steam generator (HRSG), superheated steam is generated. This steam expands in a steam turbine, which drives a generator. The steam is then condensed into water in a condenser. The cooling water circuit is modelled by a sink and cooling water pump. The condensate water from the condenser is pumped by a condensate pump to the deaerator, where it is vented from the turbine using extraction steam. Then the feed-water is pumped by a feed-water pump to the HRSG.

2.1.Heat Transfer

Choosing materials is important for heat transfer in fuel cell systems with cooling issues. It can be
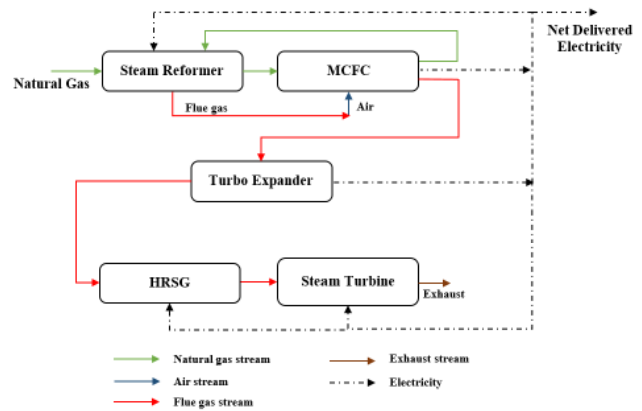

Fig.1. Schematic of the proposed hybrid cycle.

noted that if the system is a mobile electrolyte mode, cooling studies are conducted relative to electrolyte circulation.

Heat transfer in fuel cell systems with cooling issues and for choosing materials is important. It can be noted that if the system is a mobile electrolyte mode, cooling studies are in relation with electrolyte circulation.So, according to the rate of heat production in electrochemical reactions and selected materials as electrodes and walls (which transfer part of the produced heat to the environment), electrolyte circulation flow rate can be set somehow that eject the waste heat from system.Furthermore, system performance temperature should be kept constant, in the ideal amount [15,16].According to choice the control volumes, heat transfer equations can apply to various parts or whole of system [17].

3. System Modeling and Simulation

Utilizing Cycle-Tempo software, the development and numerical simulation of the proposed hybrid system is performed [28]. All the elements of this hybrid system (i.e. gas turbine, compressor, MCFC unit, heat exchangers, etc.) have been completely simulated. The simulated cycle is shown in Fig. 2.

3.1.Model Assumptions

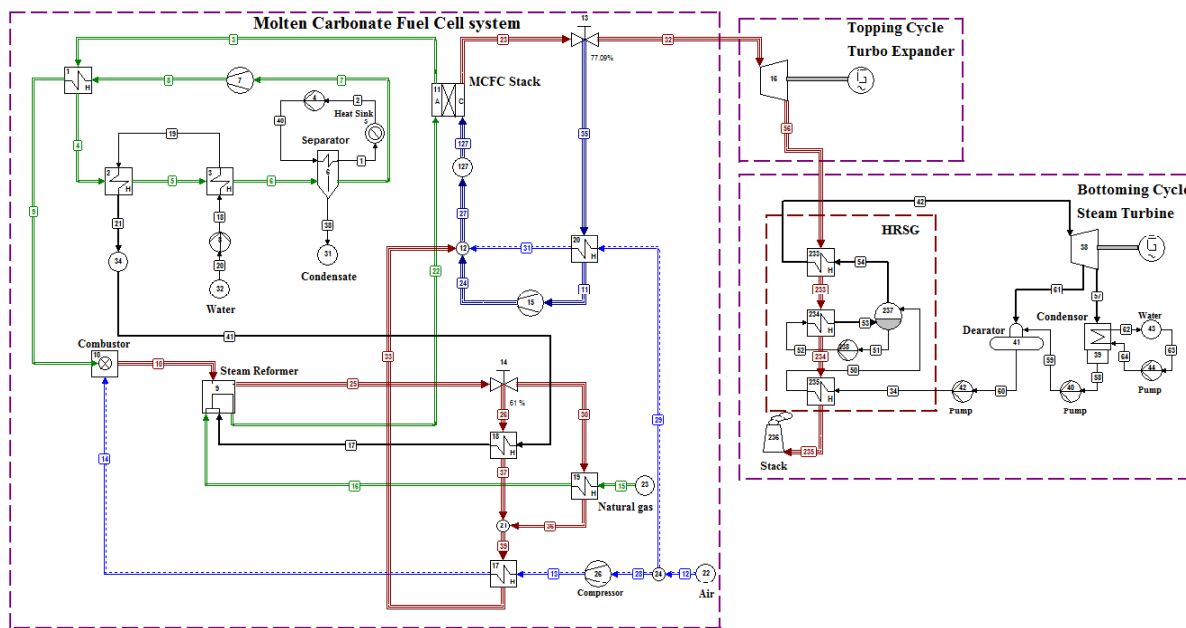The following general assumptions have been made

Fig. 2. MCFC-Turbo expander-Steam turbine hybrid cycle.

regarding all the apparatus:

1. The apparatus are operated in steady state.

2. The heat exchangers are operating in counter current flow.

3. The processes are adiabatic.

4. The reforming reactions occur at a constant temperature.

For the base case, simulation of this hybrid system is carried out by keeping the mean current density and cell area of the MCFC fixed at 1500 A/m^2 and 750 m^2, respectively.

The composition of the natural gas used in the proposed hybrid cycle is shown in Table 2.

Table 2. Composition of the natural gas.

Component	Mole (%)
C_2H_6	2.87
C_3H_8	0.38
C_4H_{10}	0.15
C_5H_{12}	0.04
C_6H_{14}	0.05
CH_4	81.29
CO_2	0.89
N_2	14.32
O_2	0.01
LHV (kJ/kg)	37998.9

Additionally, in Table 3 input parameters to the

MCFC section are shown while input parameters to the turbo expander and steam turbine sections are shown in Table 4.

Table 3. Input parameters of externally reformed MCFC unit

Parameter	Value (unit)
Fuel utilization factor	0.71
MCFC Reaction pressure	8 (bar)
MCFC Reaction temperature	650 (°C)
Stack area	750 (m^2)
Cell resistance	6.089×10^{-5} (Ω)
DC/AC conversion efficiency	0.96
Anode and cathode inlet temperature	600 (°C)
Steam reformer reaction pressure	8 (bar)
Steam reformer reaction temperature	800 (°C)

Table 4. Input parameters of turbo expander and steam turbine sections

Parameter	Value (unit)
Turbo expander isentropic efficiency	0.75
Expansion ratio of the turbo expander	6
Generator efficiency of TE	0.95
Steam turbine isentropic efficiency	0.8
Outlet pressure of ST feed-water pump	80 (bar)
Steam drum circulation ratio	4

3.2. MCFC section modeling

The MCFC unit used in this hybrid system is

reformed externally. The reformer, placed upstream of the fuel cell system, is used to convert natural gas into hydrogen rich stream. Steam used in the reformer and the heat required for the reforming reaction is acquired from the anode outlet, which is combusted before it enters the reformer. The MCFC model is used to calculate the performance of the fuel cell as a function of parameters that are controlled by fuel cell operators. These control parameters include the total fuel utilization and the current density. Fuel utilization is the degree of fuel conversion that is fed into the cell. General characteristics of this available MCFC model are [1]:

This model can be suitable for stacks of both tubular and flat plate cells. .

The model is isothermal, i.e. the calculated chemical balances on the active cell area and the current density are based on the average cell temperature.

The MCFC stack consists of a number of cells connected in series, with identical performance.

The processes occurring inside the fuel cell are modeled as follows [1, 28]:

The mass balance over the apparatus is:

$$\phi_{m,a,in} + \phi_{m,c,in} - \phi_{m,a,out} - \phi_{m,c,out} = 0 \tag{1}$$

The equation that describes the mass exchange between cathode and anode is:

$$\phi_{m,a,in} - \phi_{m,a,out} = -\phi_{m,c \to a} \tag{2}$$

It is assumed that all of the processes occur at constant temperature and pressure (Pcell and Tcell), which are the average cell pressure and temperature. For complete conversion of all the fuel components in the fuel cell, the current through the fuel cell is given as [1]:

$$I_F = \frac{\phi_{m,a,in}}{M_{mol,a}} \times \left(y_{H_2}^0 + y_{CO}^0 + y_{CH_4}^0 \right) \times 2F \tag{3}$$

Where, y_i^0 are the concentrations at the inlet and M_{mol} is the molecular mass of the anode gas. In reality, only part of the fuel in the fuel cell is converted. If the ratio between the real and the maximum conversion

is specified by the utilization level U_F, then the real current through the cell is given as [1, 28]:

$$I = I_F \times U_F \tag{4}$$

Total mass flow O_2 from cathode to anode is given by [29]:

$$\phi_{O_2,c \to a} = M_{mol,O_2} \times \frac{I}{4F} \tag{5}$$

CO_2 transported from the cathode to the anode is given by [29]:

$$\phi_{CO_2,c \to a} = M_{mol,CO_2} \times \frac{I}{2F} \tag{6}$$

The composition at the cathode outlet are now calculated from the mole balances for the components at the cathode. Similarly, the quantities of H_2 and CO that are converted on the cell area are calculated from the current 'I'.

Here a one-dimensional model is considered, i.e. the temperatures, pressures, and compositions are supposed to be constant in a cross-section, perpendicular to the direction of the fuel cell flow. For the processes that occur without losses within the fuel cell, the cell voltage is identical to the reversible voltage or Nernst voltage 'E_r' and is given as [10]:

$$E_r = E_T^0 + \frac{RT_{cell}}{2F} \ln \left\{ \frac{y_{O_2,c}^{1/2} \, y_{H_2,a} \, y_{CO_2,c}}{y_{H_2O,a} \, y_{CO_2,a}} \times P_{cell}^{1/2} \right\} \tag{7}$$

Where, E_T^0 is the standard reversible voltage for hydrogen, which only depends on the temperature, and is calculated from the change in the Gibbs energy 'ΔG' as [1]:

$$E_T^0 = + \frac{\Delta G_T^0}{2F} \tag{8}$$

In reality, the processes in the cell occur irreversibly, and hence the cell voltage 'V_x' is smaller than the reversible voltage. The difference between reversible and real voltage is indicated here with the voltage loss ΔV_x as [1]:

$$V_x = E_r - \Delta V_x \tag{9}$$

In the model, it is assumed that the voltage losses on the level of the electrodes are negligible in the x-direction. This means that the cell voltage is supposed to be constant over the fuel cell. Hence, the overall voltage is [1]:

$$V = E_r - \Delta V_x \tag{10}$$

The voltage loss can be regarded as the driving force for the reactions in the fuel cell, and thus for the current density. Hence, it can be assumed that the current density is proportional to the voltage loss. By analogy with Ohm's law, the proportionality constant is indicated with the equivalent cell resistance 'R$_{eq}$'. For cross section x, current density is:

$$i_x = \frac{\Delta V_x}{R_{eq}} \tag{11}$$

Finally, the velocity with which H$_2$ is converted in a cross-section x, can be calculated from the current density as [28, 29]:

$$\frac{dn_{H_a}}{dx} = \frac{i_x}{2F} \tag{12}$$

The changes in the concentrations of the components are calculated using the above equation, the mole balances for the components and the reaction balances for shift reactions. On the basis of the given equations, the voltage and current density are calculated in a cross-section with the help of numerical methods. The electrical output power of the fuel cell stack is given as:

$$P_e = V \times I \times \eta_{DC-AC} \tag{13}$$

3.1. Turbo Expander Modeling

Roger and Mayhew's method has been considered to model the turbo expander [30]. This method, explained below, is considered for a specific heat coefficient (C$_p$) and isentropic index (γ) in the whole process or for parts of the process. Basically, these data are used to calculate the isentropic efficiency. However, is the study provides a provision to supply the isentropic efficiency by turbine characteristics from previous studies [4, 30]. To calculate the specific enthalpies at the extractions, straight expansion lines in the Mollier diagram are considered between inlet and outlet conditions.

According to the above description, the outlet temperature of the turbo expander has been estimated using Eq. (14) [30].

$$T_4 = T_3 - T_3 \times \eta_t \times \left[1 - \frac{1}{R_t} \right]^{\frac{\gamma-1}{\gamma}} \tag{14}$$

Where, η_t is the isentropic efficiency of the turbo expander and R$_t$ is the expansion ratio.

Additionally, work of turbine is calculated by Eq. (15) as follows [30]:

$$W_t = C_p \times (T_3 - T_4) \tag{15}$$

3.2. Steam Turbine Cycle Modeling

The steam turbine bottoming cycle has been modeled based on the Rankine cycle methodology. In this section, the mean temperature at which heat is supplied is less than the maximum temperature, so that the efficiency is less than that of a Carnot cycle working between the same maximum and minimum temperatures. To model this cycle the primary energy absorbed by the boiler, the power produced by the generator, the electricity consumption of the pumps, and the net supplied power have been indicated. It should be mentioned that the pumps electricity consumption are considered as auxiliary power consumers, which when subtracted from gross electricity generated estimate the net power delivered.

Input and output works have been defined to examine the efficiency of the Rankine cycle, so the thermal efficiency can be written as follows [30, 13]:

$$\eta_{thermal, ST} = \frac{W_{out} - W_{in}}{Q_{in}} \tag{16}$$

Where, W$_{out}$ and W$_{in}$ are generated power and pumps

work, respectively. Also, Q_{in} is the input heat to the cycle.

3.3. Moisture Separator Modeling

In the moisture separator, the incoming gas is cooled by a cooling medium flowing in the opposite direction, as a result of which water vapor condenses. The condensate formed is collected and discharged via a separate pipe. The three mass equations (mass balance, secondary equation of the cooling medium and the equation for the quantity of condensate separated, i.e. the specified mass equation) and the energy equation of the cooler have been used in the system modeling, to calculate mass flows.

4. Exergy Analysis

In the proposed cycle, greater use of thermal energy and waste reduction in the plant was considered to enhance total efficiency. As observed in Eq. (17) , the total cycle efficiency is obtained from the sum of electrical and thermal efficiencies of the system. The electrical efficiency of the system is achieved from the MCFC, turbo expander and steam turbine electrical efficiencies using the general Eq. (18) [29, 30]. The total exergetic efficiency of the system is calculated by Eq. (19) and is shown in Table 5.

$$\eta_{total} = \eta_{electrical} + \eta_{heat} \tag{17}$$

$$\eta_{electrocal} = \frac{total\ power\ generated}{fuels'\ LHV} \tag{18}$$

5. Results and Discussions

Simulation of this hybrid system allows the evaluation of mass flow-rate, power output, exergy efficiency and energy values across the different components of the system. For the system, it is observed that a net electrical exergy efficiency of 71.0% is achieved when a steam/fuel ratio of 2.59

is kept for the reformer, and a fuel utilization of 71% is achieved for the MCFC. This is the base case performance for the system. In the cathode of the MCFC, cathode recycling and steam reformer exhaust are fed along with fresh air to the cathode inlet. In addition, recycled anode exhaust stream is fed to the combustor of reformer at 460°C after being enriched by CO_2 in the moisture separator. Both the anode and cathode off-gasses leave the MCFC at 700°C. The electrical power output from the turbo expander is about 218 kW, while the MCFC delivers about 948 kW of electricity. Using the turbo expander exhaust stream, hot steam is produced in the HRSG. This steam is then used for cogeneration around 55.5 kW through the steam turbine cycle.

For this kind of exergy analysis it is important to have available exergy values of process flows and exergy losses in the apparatuses, as well as exergy efficiencies of the apparatuses. Exergy analysis of this hybrid cycle has been performed based on the equations shown in Table 5 [1, 2].

In Fig. 3, variation of total exergy efficiency of the plant with increasing fuel utilization is plotted for a steam/fuel ratio of 2.59% for the steam reformer. Feasible range of utilization factor is 59%-71% for this system, so a maximum total exergy efficiency of 68.74% is achieved for 71% fuel utilization.

The base case performance for the hybrid system is shown in Table 6.

Based on presented calculations, the proposed cycle has higher efficiency in compare with previous studies. Main results of the previous studies have been shown in Table 1. Comparing results of different researches using quantitative approach, is usual.

One of the advantages of the recommended cycle, as presented in Fig. 4, is its low sensitivity to ambient temperature changes. Where ambient temperature increases for each degree of Celsius, the output power decreases about 0.02% in comparison with gas turbines [30]. Therefore, this cycle can be a suitable alternative to conventional hybrid systems in tropical areas, where the delivered power of combined cycles shows a remarkable decrease. This cycle has been modeled for the Tehran, Iran climate, so the averages

Table 5. Exergy equations in cycle simulation [1, 7, 29, 30].

Element	Exergy Efficiency	Equation No.
General definition of functional efficiency	$\eta_{Ex,f} = \dfrac{\sum Ex_{product}}{\sum Ex_{source}}$	(19)
Electrical exergy efficiency of hybrid system	$\eta_{Ex,electrical} = \dfrac{\sum E_{electrical,out} - \sum E_{electrical,in}}{Ex_{fuel}}$	(20)
Total exergy efficiency of hybrid system	$\eta_{Ex,total} = \dfrac{\sum \eta_{electrical,out} + \sum Ex_{heat,out} - \sum P_{electrical,in}}{Ex_{fuel,in}}$	(21)
Exergy efficiency of fuel cell	$\eta_{Ex,f(fuel\;cell)} = \dfrac{E_{electrical}}{(Ex_{fuel,in} - Ex_{fuel,out}) + Ex_{ox,in} - Ex_{ox,out}}$	(22)
Exergy efficiency of turbine	$\eta_{Ex,f(turbine)} = \dfrac{E_{shaft}}{Ex_{in} - \sum Ex_{out}}$	(23)
Exergy efficiency of steam reformer	$\eta_{Ex,f(reformer)} = \dfrac{Ex^{ch}_{product\;gas} - Ex^{ch}_{steam} - Ex^{ch}_{feed}}{(Ex^{tm}_{flue\;gas,in} - Ex^{tm}_{flue\;gas,out}) - (Ex^{tm}_{product\;gas} - Ex^{tm}_{steam} - Ex^{tm}_{feed})}$	(24)
Exergy efficiency of heat exchanger	$\eta_{Ex,f(heat\;exchanger)} = \dfrac{Ex_{p,out} - Ex_{p,in}}{Ex_{s,out} - Ex_{s,in}}$	(25)
Exergy efficiency of drum	$\eta_{Ex,f(drum)} = \dfrac{Ex_{steam,out} - Ex_{steam,in}}{Ex_{evaporator,out} - Ex_{evaporator,in}}$	(26)
Exergy efficiency of combustion chamber	$\eta_{Ex,f(combustion\;chamber)} = \dfrac{Ex^{tm}_{flue\;gas} - Ex^{tm}_{fuel} - Ex^{tm}_{ox}}{Ex^{ch}_{fuel} + Ex^{ch}_{ox} - Ex^{ch}_{flue\;gas}}$	(27)
Exergy efficiency of compressor, pump	$\eta_{Ex,f(compressor,\;pump)} = \dfrac{Ex_{out} - Ex_{in}}{Ex_{shaft}}$	(28)

Table 6. Results of simulation for the proposed hybrid system in base case.

Parameter	Value (unit)
Fuel flow rate	0.043 (kg/s)
Turbo expander inlet temperature	973.15 (K)
MCFC delivered power	940.97 (kW)
Turbo expander delivered power	218.7 (kW)
Steam turbine delivered power	55.54 (kW)
Auxiliary power consumption	97.20 (kW)
Net electrical power output	1125.05 (kW)
Delivered heat	59.34 (kW)
Gross electrical exergy efficiency	71.00 (%)
Net electrical exergy efficiency	65.35 (%)
Total exergy efficiency	68.74 (%)
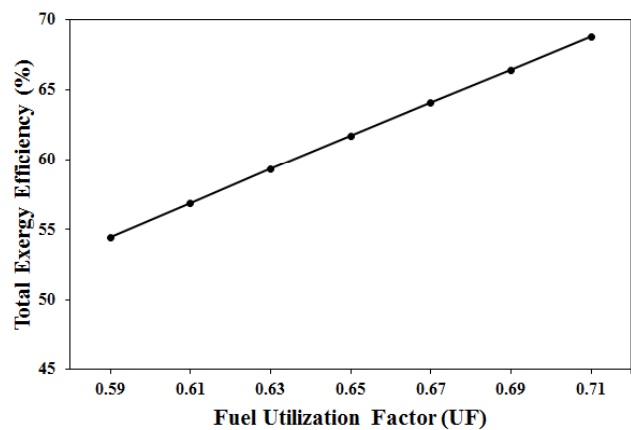
Fig. 3. Variation of total exergy efficiency of the proposed hybrid system with steam/fuel ration of 2.59% for feasible range of fuel utilization.
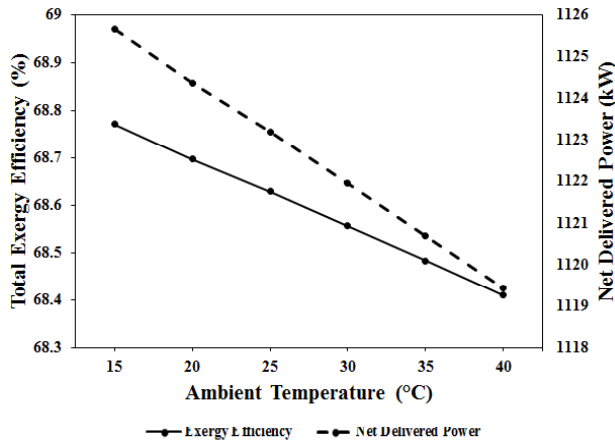
Fig. 4. Variation of total exergy efficiency and net delivered power of the proposed hybrid system for ambient temperature and relative humidity changes of Tehran, Iran.

of ambient temperature and relative humidity in Tehran are shown in Table 7.

Fig. 5 represents the cell voltage and the total exergy efficiency vs. current density at a fuel cell operating temperature of 650°C. An increase in the current density incurs lower operating voltage due to the electric losses, which also can be concluded from Eq. (11).

Table 7. Averages of ambient temperature and relative humidity in Tehran, Iran [31].

Ambient Temperature (°C)	Relative Humidity (%)
15	30
20	28
25	22
30	19
35	17
40	15

As a result, higher current densities lead to a higher rate of exergy destruction of the fuel cell which comprises the largest contribution to the total exergy destruction of the plant and subsequently deteriorates the total exergy efficiency of the hybrid cycle.

According to Table 6, using a turbo expander and steam turbine along with heat recovery in this hybrid cycle caused a higher exergy efficiency when compared with previous studies.

Exergy efficiencies in each main part of the proposed cycle along with their numbers from Fig. 2, are shown in Table 8. The major exergy destructions have been indicated for equipment such as combustor, reformer and heat exchangers. For some apparatuses, such as pumps and compressors, exergy losses are negligibleas shown by low energy consumption.
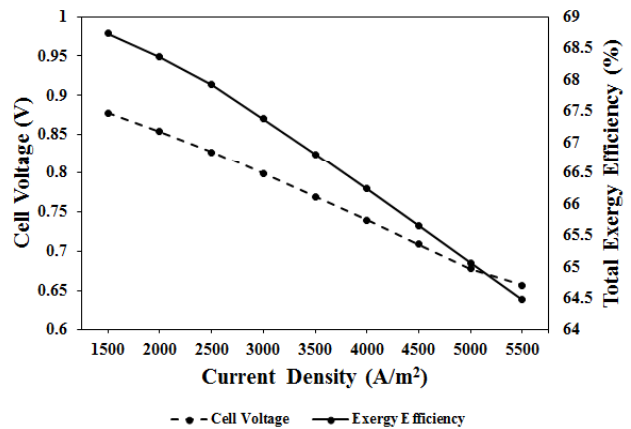

Fig 5. Effect of current density variations on exergetic efficiency.

Table 8. Calculated exergy efficiencies of main elements of the proposed cycle.

Apparatus (No.)	Exergy Efficiency (%)
Turbo Expander (16)	87.43
Steam Turbine (38)	80.40
MCFC (11)	93.04
Compressor (7)	57.97
Compressor (15)	76.80
Compressor (26)	76.50
Reformer (9)	80.48
Pump (4)	44.43
Pump (8)	55.10
Pump (40)	45.37
Pump (42)	49.40
Pump (44)	55.54
Pump (238)	86.43
Combustion chamber (10)	76.10
Heat Exchanger (1)	67.96
Heat Exchanger (2)	66.87
Heat Exchanger (3)	80.46
Heat Exchanger (17)	88.92
Heat Exchanger (18)	75.89
Heat Exchanger (19)	64.37
Heat Exchanger (20)	65.64
Heat Exchanger (233)	66.11
Heat Exchanger (235)	66.47

Delivered heat is achieved from the considered heat sink in the moisture separator section. Inlet and outlet temperatures of this unit are 80 and 60°C, respectively. Exergy efficiency visualizes the thermodynamic significance of the heat produced [32]. Since the exergy of heat depends on the temperature, and is for finite temperatures always smaller than the energy quantity, exergy efficiencies of combined heat and power plants will usually be lower than comparable thermal efficiencies. The difference is determined specifically by the temperature level of the heat produced.

6.Conclusion

In this study, a MCFC-Turbo expander-steam turbine novel hybrid system was proposed to attain high power generation capacity in conventional MCFC combined cycles while maintaining reasonable total plant exergy efficiency. The following conclusions can be drawn from this study:

• Maximum performance of a plant with electrical exergy efficiency of 71.0% has been achieved at a steam/fuel ratio of 2.59 and 71% fuel utilization.

• Around 55.5 kW of electricity is obtained by cogeneration from this plant when operated at the base case situation.

• The total exergy efficiency (electrical and heat) of the system is 68.74%.

• Increase in the rate of fuel utilization factor of the MCFC (at a feasible range), indicated a remarkable increase in total exergy efficiency.

• In ambient temperature changes from 15 to 40°C, the generated power decreases to about 0.5%, while it is significantly higher in gas turbine or steam turbine cycles.

• Increase in current density value of the MCFC caused an increase in electric losses and exergy destruction of the hybrid system.

Nomenclature

$c{\rightarrow}a$ From Cathode to Anode

C_p	Specific Heat Coefficient [kJ/kg °C]
E_T^0	Standard Reversible Voltage [V]
E_r	Nernst Voltage [V]
F	Faraday Constant [C]
ΔG_T^0	Standard Gibbs Energy Change [kJ/mol]
I	Current [A]
i_x	Current Density [A.m^2]
LHV	Lower Heating Value [kJ kg^{-1}]
M_{mol}	Molecular Mass [kg/mol]
P	Pressure [bar]
P_e	Power [kW]
Q	Heat [kJ]
R_{eq}	Equivalent Cell Resistance [Ω]
R_t	Expansion Ratio [-]
T	Temperature [°C]
U_F	Utilization Factor [-]
V	Overall Voltage [V]
V_x	Cell Voltage [V]
W	Work [kJ]
y_i^0	Concentrations at the Inlet

Abbreviations

CHP	Combined Heat and Power
Eff	Efficiency
En	Energy
Ex	Exergy
GT	Gas Turbine
HRSG	Heat Recovery Steam Generator
MCFC	Molten Carbonate Fuel Cell
SOFC	Solid Oxide Fuel Cell
ST	Steam Turbine
STIG	Steam Injection Gas turbine
TE	Turbo Expander
Greek	
$\eta_{(DC-AC)}$	Efficiency of DC/AC Conversion [%]
η	Efficiency [%]
φ_m	Mass Flow [kg/sec]
γ	Isentropic Index [-]

Subscripts

a	Anode
c	Cathode

cell	Cell
ch	Chemical
electrical	Electrical
F	Faraday
f	Functional
Fuel	Fuel
heat	Heat
in	Inlet
out	Outlet
ox	Oxidant
p	Primary Flow
Product	Product
s	Secondary Flow
shaft	Shaft Power
Source	Source
ST	Steam Turbine
T	Temperature
t	Turbo Expander
thermal	Thermal
tm	Thermo-Mechanical
total	Total

References

[1] Williams, M.C., 7th ed., Fuel Cell Handbook, EG&G Technical Services, Inc., 2004.

[2] Ozgoli, H.A., Ghadamian, H., Roshandel, R., Moghadasi, M., "Alternative Biomass Fuels Consideration Exergy and Power Analysis for a Hybrid System Includes PSOFC and GT Integration", Energy Sources, Part A: Recovery, Utilization, and Environmental Effects, 2015, 37: 1962.

[3] Ozgoli, H.A., Ghadamian, H., Farzaneh, H., "Energy Efficiency Improvement Analysis Considering Environmental Aspects in Regard to Biomass Gasification PSOFC-GT Power Generation System", Procedia Environmental Sciences, 2013, 17: 831.

[4] Ghadamian, H., Hamidi, A.A., Farzaneh, H., Ozgoli, H.A., "Thermo-Economic Analysis of Absorption Air Cooling System for Pressurized Solid Oxide Fuel Cell/Gas Turbine Cycle", Journal of Renewable and sustainable Energy, 2012, 4: 043115.

[5] Ozgoli, H.A., Ghadamian, H., Hamidi, A.A., "Modeling SOFC & GT Integrated-Cycle Power System with Energy Consumption Minimizing Target to Improve Comprehensive cycle Performance (Applied in pulp and paper, case studied)", International Journal of Engineering Technology, 2012, 1: 6.

[6] Ozgoli, H.A., Moghadasi, M., Farhani, F., Sadigh, M. "Modeling and Simulation of an Integrated Gasification SOFC-CHAT Cycle to Improve Power and Efficiency", Environmental Progress & Sustainable Energy, 2016, DOI: 10.1002/ep.12487.

[7] Rashidi, R., Dincer, I., Berg P., "Energy and exergy analysis of a hybrid molten carbonate fuel cell system", Journal of Power Sources, 2008, 185:1107.

[8] De Simon, G., Parodi F., Fermeglia, M., Taccani, R., "Simulation of process for electrical energy production based on molten carbonate fuel cells", Journal of Power Sources, 2003, 115: 210.

[9] Carapellucci, R., Saia, R., Giordano, L., "Study of Gas-Steam Combined Cycle Power Plants Integrated with MCFC for Carbon Dioxide Capture", Energy Procedia, 2014, 45: 1155.

[10] Rashidi, R., Berg P., Dincer, I., "Performance investigation of a combined MCFC system", International Journal of Hydrogen Energy, 2009, 34: 4395.

[11] Campanari, S., Manzolini, G., Chiesa, P., "Using MCFC for High Efficiency CO2 Capture from Natural Gas Combined Cycles: Comparison of Internal and External Reforming", Applied Energy, 2013, 112: 772.

[12] Sciacovelli, A., Verda, V., "Sensitivity Analysis Applied to the Multi-Objective Optimization of a MCFC Hybrid Plant", Energy Conversion and Management, 2012, 60: 180.

[13] Hazarika, M.M., Ghosh, S., "Simulated Performance

Analysis of a GT-MCFC Hybrid System Fed with Natural Gas", International Journal of Emerging Technology and Advanced Engineering, 2013, 3, Special Issue 3: 292.

[14] Liu, A., Wang, B., Zeng, W., Chen, B., Weng, Y., "Catalytic Combustion and System Performance Assessment of MCFC-MGT Hybrid System", International Journal of Hydrogen Energy, 2014, 39: 7437.

[15] Orecchini, F., Bocci, E., Di Carlo, A., "MCFC and micro Turbine Power Plant Simulation", Journal of Power Sources, 2006, 160: 835.

[16] Liu, A., Weng, Y., "Performance Analysis of a Pressurized Molten Carbonate Fuel Cell/micro-Gas Turbine Hybrid System", Journal of Power Sources, 2010, 195: 204.

[17] McLarty, D., Brouwer, J., Samuelsen, S., "Fuel Cell – Gas Turbine Hybrid System Design Part I: Steady State Performance", Journal of Power Sources, 2014, 257: 412.

[18] Karvountzi, G.C., Price C.M., Duby P.F., "Comparison of Molten Carbonate and Solid Oxide Fuel Cells for Integration in a Hybrid System for Cogeneration or Tri-generation", Proceedings of IMECE04, ASME International Mechanical Engineering Congress and Exposition, Anaheim, California, USA, November 13-20, 2004.

[19] Azegami, O., "MCFC/MGT Hybrid Generation System", Special Issue Core Technology of Micro Gas Turbine for Cogeneration System, R&D Review of Toyota CRDL, 2006, 41: 36.

[20] Huang, H., Li J., He, Z., Zeng, T., Kobayashi, N., Kubota, M., "Performance Analysis of a MCFC/MGT Hybrid Power System Bi-Fueled by City Gas and Biogas", Energies, 2015, 8: 5661.Azegami, O., "MCFC/MGT Hybrid Generation System", Special Issue Core Technology of Micro Gas Turbine for Cogeneration System, R&D Review of Toyota CRDL, 2006, 41: 36.

[21] Leto, L., Dispenza, C., Moreno, A., Calabr, A., "Simulation Model of a Molten Carbonate Fuel Cell - micro Turbine Hybrid System", Applied Thermal Engineering,

2011, 31, 1263.

[22] El-Emam, R.S., Dincer, I., "Energy and Exergy Analyses of a Combined Molten Carbonate Fuel Cell - Gas Turbine System", International journal of hydrogen energy, 2011, 36: 8927.

[23] Rashidi, R., Berg, P., Dincer, I., "Performance Investigation of a Combined MCFC System", International Journal of Hydrogen Energy, 2009, 34: 4395.

[24] Chacartegui, R., Blanco, M.J., Mu~noz de Escalona, J.M., Sanchez D., Sanchez T., "Performance Assessment of Molten Carbonate Fuel Cell-Humid Air Turbine Hybrid Systems", Applied Energy, 2013, 102: 687.

[25] Haseli, Y., Dincer, I., Naterer, G.F., Thermodynamic Analysis of a Combined Gas Turbine Power System with a Solid Oxide Fuel Cell through Exergy", Thermochimica Acta, 2008, 480: 1.

[26] Varbanov, P.S., Kleme, J., Shah, R.K., Shihn, H., "Power Cycle Integration and Efficiency Increase of Molten Carbonate Fuel Cell Systems", Journal of Fuel Cell Science and Technology, 2006, 3: 375.

[27] Haghighat Mamaghani, A., Najafi, B., Shirazi, A., Rinaldi, F., "Exergetic, Economic, and Environmental Evaluations and Multi-Objective Optimization of a Combined Molten Carbonate Fuel Cell-Gas Turbine System", Applied Thermal Engineering, 2015, 77: 1.

[28] Advanced Simulation for Power and Total Energy systems (ASIMPTOTE), Delft, Netherlands, http://www.asimptote.nl/software/cycle-tempo/

[29] Wester, W., "Computer Program for Fuel Cell Systems)", Report EV- 1464, Delft University of Technology, Laboratory for Thermal Power Engineering, 1987.

[30] Razak, A.M.Y., Industrial Gas Turbines Performance and Operability, Woodhead Publishing Ltd., Oxford, UK, 2007.

[31] https://weatherspark.com/averages/32810/Tehran-Iran

[32] Koras, T.J., "Exergy Criteria of Performance for Thermal Plant: Second of Two Papers on Exergy Techniques in Thermal Plant Analysis", International Journal of Heat and Fluid Flow, 1980, 2:147.